

Fixed point scenario in the Two Higgs Doublet Model inspired by degenerate vacua.

C. D. Froggatt^a, R. Nevzorov^{a 1}, H. B. Nielsen^b, D. Thompson^a

^a *Department of Physics and Astronomy,*

Glasgow University, Glasgow, Scotland

^b *The Niels Bohr Institute, Copenhagen, Denmark*

Abstract

We consider the renormalisation group flow of Higgs and Yukawa couplings within the simplest non-supersymmetric two Higgs doublet extension of the Standard Model (SM). In this model the couplings are adjusted so that the multiple point principle (MPP) assumption, which implies the existence of a large set of degenerate vacua at some high energy scale Λ , is realised. When the top quark Yukawa coupling at the scale Λ is large, the solutions of RG equations in this MPP inspired 2 Higgs Doublet Model (2HDM) converge to quasi-fixed points. We analyse the Higgs spectrum and couplings in the quasi-fixed point scenario and compute a theoretical upper bound on the lightest Higgs boson mass. When the scale Λ is low, the coupling of the SM-like Higgs scalar to the top quark can be significantly larger in the considered model than in the SM, resulting in the enhanced production of Higgs bosons at the LHC.

¹ On leave of absence from the Theory Department, ITEP, Moscow, Russia

1. Introduction

A quasi-fixed point solution [1]–[2] is one of the most spectacular features of the renormalisation group (RG) equations. The existence of a quasi-fixed point implies that the solutions of the RG equations, corresponding to a range of different initial values of fundamental parameters at a high energy scale, are focused in a narrow interval in the infrared region. This allows us to get some predictions for couplings and physical observables at low energy scales. However such predictions are not always compatible with the existing experimental data. For example, within the Standard Model (SM) the quasi-fixed point solution leads to an unacceptably large mass for the top-quark which disagrees with the results of experimental measurements obtained at FNAL.

This problem can be overcome within supersymmetric (SUSY) and non-supersymmetric two Higgs doublet extensions of the SM. The most general renormalizable scalar potential of the model involving two Higgs doublets is given by

$$\begin{aligned}
 V_{eff}(H_1, H_2) = & m_1^2 H_1^\dagger H_1 + m_2^2 H_2^\dagger H_2 - \left[m_3^2 H_1^\dagger H_2 + h.c. \right] + \\
 & \frac{\lambda_1}{2} (H_1^\dagger H_1)^2 + \frac{\lambda_2}{2} (H_2^\dagger H_2)^2 + \lambda_3 (H_1^\dagger H_1) (H_2^\dagger H_2) + \lambda_4 |H_1^\dagger H_2|^2 + \\
 & + \left[\frac{\lambda_5}{2} (H_1^\dagger H_2)^2 + \lambda_6 (H_1^\dagger H_1) (H_1^\dagger H_2) + \lambda_7 (H_2^\dagger H_2) (H_1^\dagger H_2) + h.c. \right]
 \end{aligned} \tag{1}$$

where $H_n = \left(\chi_n^+, \frac{1}{\sqrt{2}}(H_n^0 + iA_n^0) \right)$, $n = 1, 2$. In the minimal supersymmetric standard model (MSSM) Higgs self-couplings λ_5 , λ_6 and λ_7 are zero at the tree level while the values of λ_1 , λ_2 , λ_3 and λ_4 are proportional to the gauge couplings squared. After the inclusion of loop corrections all possible Higgs self-couplings are generated and the values of the λ_i at the electroweak scale depend on the soft SUSY breaking parameters.

In the non-supersymmetric two Higgs doublet extension of the SM (2HDM) the Higgs self-couplings λ_i and the mass terms m_i^2 are arbitrary parameters. In order to suppress non-diagonal flavour transitions in the 2HDM, a certain discrete Z_2 symmetry is normally imposed. This Z_2 symmetry requires the down-type quarks to couple to just one Higgs doublet, H_1 say, while the up-type quarks couple either to the same Higgs doublet H_1 (Model I) or to the second Higgs doublet H_2 (Model II) but not both [3]¹. The custodial Z_2 symmetry forbids the mixing term $m_3^2 (H_1^\dagger H_2)$ and the Higgs self-couplings λ_6 and λ_7 . But usually a soft violation of the Z_2 symmetry by dimension-two terms is allowed, since it does not induce Higgs-mediated tree-level flavor changing neutral currents (FCNC).

At the physical minimum of the scalar potential (1) the neutral components of the

¹Due to the invariance of the Lagrangian of the 2HDM under this symmetry the leptons can only couple to one Higgs doublet as well, usually chosen to be the same as the down-type quarks.

Higgs doublets develop vacuum expectation values $\langle H_1^0 \rangle = \frac{v_1}{\sqrt{2}}$ and $\langle H_2^0 \rangle = \frac{v_2}{\sqrt{2}}$, breaking electroweak symmetry and generating masses for the bosons and fermions. In the MSSM and 2HDM of type II, the induced running t -quark mass m_t is given by

$$m_t(M_t) = \frac{h_t(M_t)v}{\sqrt{2}} \sin \beta, \quad (2)$$

where $M_t = 171.4 \pm 2.1$ GeV is the top quark pole mass [4] and $v = \sqrt{v_1^2 + v_2^2} = 246$ GeV is fixed by the Fermi scale, while $\tan \beta = v_2/v_1$ remains arbitrary. Because $\sin \beta$ can be considerably smaller than unity a phenomenologically acceptable value of $m_t(M_t)$ can be obtained even for $h_t(M_t) \gtrsim 1$, which is not the case in the SM where such large values of the top quark Yukawa coupling have already been ruled out. In the MSSM a broad class of solutions of the RG equations converges to the quasi-fixed point which corresponds to $\tan \beta \simeq 1.3 - 1.8$, resulting in a stringent constraint on the lightest Higgs boson mass $m_h \lesssim 94 \pm 5$ GeV [5]–[6]. Such a light Higgs boson has already been excluded by LEP II data. But at large $\tan \beta = 50 - 60$ the solutions of the MSSM RG equations are focused near another quasi-fixed point, which has not been ruled out by LEP measurements. The RG flow of Yukawa couplings and the particle spectrum in the vicinity of the MSSM quasi-fixed points were discussed in [6]–[7]. The quasi-fixed point scenario in the non-supersymmetric two Higgs doublet extension of the SM was studied in [2], [8].

In this letter we consider the quasi-fixed point scenario within a specific two Higgs doublet model obtained from the application of the multiple point principle (MPP) to the 2HDM of type II. The MPP postulates the existence of the maximal number of phases with the same energy density allowed by a given theory [9]. Being applied to the 2HDM of type II, the multiple point principle implies the existence of a large set of degenerate vacua at some high energy scale Λ (MPP scale). To ensure that the vacua at the electroweak and MPP scales have the same vacuum energy density, λ_5 must have zero value while $\lambda_1(\Lambda)$, $\lambda_2(\Lambda)$, $\lambda_3(\Lambda)$ and $\lambda_4(\Lambda)$ obey two MPP conditions (see [10]). Thus the MPP inspired 2HDM has less free parameters than the 2HDM of type II and therefore can be considered as a minimal non-supersymmetric two Higgs doublet extension of the SM. Also it has recently been shown that the MPP can be used to derive a softly broken custodial symmetry, which suppresses FCNC and CP violating phenomena in the 2HDM [11].

This letter is organised as follows. In the next section we examine the RG flow of $h_t(\mu)$ and $\lambda_i(\mu)$ and determine the position of the quasi-fixed points to which the solutions of the RG equations approach when $h_t(\Lambda) \gtrsim 1$. In section 3 the results obtained are used in an analysis of the Higgs masses and couplings. We establish an upper bound on the mass of the SM-like Higgs boson in the vicinity of the quasi-fixed point and argue that the Higgs production cross section at the LHC can be significantly larger in the considered model as compared with the SM. Our results are summarised in section 4.

2. RG flow of Higgs and Yukawa couplings

Let us consider the running of Higgs and Yukawa couplings in the framework of the MPP inspired 2HDM. At moderate values of $\tan\beta$ ($\tan\beta \lesssim 10$), all Yukawa couplings except the top quark one are negligibly small and can be safely ignored in our analysis of the RG flow. As a consequence the RG equations are simplified drastically and an exact analytic solution for $h_t(\mu)$ may be obtained. It can be written as follows

$$Y_t(\mu) = \frac{\frac{2E(t)}{9F(t)}}{1 + \frac{2}{9Y_t(\Lambda)F(t)}}, \quad \tilde{\alpha}_i(\mu) = \frac{\tilde{\alpha}_i(\Lambda)}{1 + b_i \tilde{\alpha}_i(\Lambda)t}, \quad (3)$$

$$E(t) = \left[\frac{\tilde{\alpha}_3(\mu)}{\tilde{\alpha}_3(\Lambda)} \right]^{8/7} \left[\frac{\tilde{\alpha}_2(\mu)}{\tilde{\alpha}_2(\Lambda)} \right]^{3/4} \left[\frac{\tilde{\alpha}_1(\mu)}{\tilde{\alpha}_1(\Lambda)} \right]^{-17/84}, \quad F(t) = \int_0^t E(\tau) d\tau,$$

where the index i varies from 1 to 3, $b_1 = 7$, $b_2 = -3$, $b_3 = -7$, $t = \ln(\Lambda^2/\mu^2)$, $\tilde{\alpha}_i(\mu) = \left(\frac{g_i(\mu)}{4\pi} \right)^2$ and $Y_t(\mu) = \left(\frac{h_t(\mu)}{4\pi} \right)^2$. Here $g_i(\mu)$ are the gauge couplings of $U(1)_Y$, $SU(2)_W$ and $SU(3)_C$ interactions. If the MPP scale is relatively high and $h_t^2(\Lambda) \gtrsim 1$ the second term in the denominator of the expression describing the evolution of $Y_t(\mu)$ is much smaller than unity at the electroweak scale. As a result the dependence of $h_t^2(M_t)$ on its initial value $h_t^2(\Lambda)$ disappears and all solutions of the RG equation for the top quark Yukawa coupling are concentrated in a narrow interval near the quasi-fixed point [1]–[2]:

$$Y_{\text{QFP}}(M_t) = \frac{2E(t_0)}{9F(t_0)}, \quad (4)$$

where $t_0 = \ln(\Lambda^2/M_t^2)$. Formally a solution of this type can be obtained in the limit when $Y_t(\Lambda)$ is infinitely large. But in reality the convergence of the RG solutions to the quasi-fixed point (4) does not require extremely large values of the top quark Yukawa coupling at the MPP scale if Λ is high enough. In Figs. 1a and 1b we plot the RG flow of the top quark Yukawa coupling for different initial values at the scale $\Lambda \simeq M_{Pl}$ and $\Lambda \simeq 10^{13} \text{ GeV}$ respectively. One can see that in both cases the solutions of the RG equations are focused in the close vicinity of the quasi-fixed point at the electroweak scale if $h_t^2(\Lambda) \gtrsim 1$ ².

The convergence of the RG solutions to the quasi-fixed point allows us to predict $h_t(M_t)$ for each fixed value of the MPP scale. Then using Eq. (2) one can find the $\tan\beta$ that corresponds to the quasi-fixed point (4). Here we use the relationship between the t -quark pole (M_t) and running ($m_t(\mu)$) masses [12]

$$m_t(M_t) = M_t \left[1 - 1.333 \frac{\alpha_s(M_t)}{\pi} - 9.125 \left(\frac{\alpha_s(M_t)}{\pi} \right)^2 \right]. \quad (5)$$

²The solutions of the RG equations also converge to a quasi-fixed point at large $\tan\beta = 50 - 60$. However this quasi-fixed point scenario leads to an unacceptably large $m_t(M_t) \gtrsim 200 \text{ GeV}$ (see [11]).

to determine $m_t(M_t)$ within the \overline{MS} scheme. We find that in the two-loop approximation $m_t(M_t) \simeq 161.6 \pm 2 \text{ GeV}$. In Table 1 we examine the dependence of the values of $h_t(M_t)$ and $\tan \beta$ corresponding to the quasi-fixed point (4) on the MPP scale. From Table 1 it becomes clear that $h_t(M_t)$ varies from 1.3 to 2 when the scale Λ changes from M_{Pl} to 10 TeV. Because the quasi-fixed point solution represents the upper bound on $h_t(M_t)$, the value of $\tan \beta$ derived from Eq. (2) should be associated with a lower bound on $\tan \beta$. Then from Table 1 one can see that the lower limit on $\tan \beta$ reduces from 1.1 to 0.5, when Λ varies from M_{Pl} to 10 TeV.

It turns out that at large values of $h_t(\Lambda) \gtrsim 1.5$, the allowed range of the Higgs self-couplings at the MPP scale is quite narrow. Stringent constraints on $\lambda_i(\Lambda)$ come from the MPP conditions. The MPP scale vacua have small vacuum energy densities ($\ll \Lambda^4$), as needed to achieve the degeneracy of these vacua and the physical one, only if the Higgs self-couplings obey the MPP conditions

$$\lambda_3(\Lambda) = -\sqrt{\lambda_1(\Lambda)\lambda_2(\Lambda)} - \lambda_4(\Lambda), \quad (6)$$

$$\begin{aligned} \lambda_4^2(\Lambda) = & \frac{6h_t^4(\Lambda)\lambda_1(\Lambda)}{(\sqrt{\lambda_1(\Lambda)} + \sqrt{\lambda_2(\Lambda)})^2} - 2\lambda_1(\Lambda)\lambda_2(\Lambda) \\ & - \frac{3}{8} \left(3g_2^4(\Lambda) + 2g_2^2(\Lambda)g_1^2(\Lambda) + g_1^4(\Lambda) \right), \end{aligned} \quad (7)$$

where $\lambda_4(\Lambda) < 0$. Thus, in contrast to the 2HDM of type II, the Higgs self-couplings $\lambda_3(\Lambda)$ and $\lambda_4(\Lambda)$ in the MPP inspired two Higgs doublet extension of the SM are determined by $\lambda_1(\Lambda)$, $\lambda_2(\Lambda)$ and $h_t(\Lambda)$. These three parameters determine the RG flow of all the couplings in the considered model. Since $\lambda_4(\Lambda)$ is a real quantity, Eq. (7) limits the allowed range of $\lambda_1(\Lambda)$ and $\lambda_2(\Lambda)$ from above. For instance, when $\lambda_1(\Lambda) = \lambda_2(\Lambda) = \lambda_0$ the value of $\lambda_4^2(\Lambda)$ remains positive only if $\lambda_0 < \frac{\sqrt{3}}{2}h_t^2(\Lambda)$.

The lower bound on the Higgs self-couplings originates from the vacuum stability conditions:

$$\lambda_1(\mu) > 0, \quad \lambda_2(\mu) > 0, \quad \tilde{\lambda}(\mu) = \sqrt{\lambda_1(\mu)\lambda_2(\mu)} + \lambda_3(\mu) + \min\{0, \lambda_4(\mu)\} > 0. \quad (8)$$

The conditions (8) must be fulfilled everywhere from the electroweak scale to the MPP scale. Otherwise another minimum of the Higgs effective potential with a huge and negative vacuum energy density arises at some intermediate scale, destabilising the physical and MPP scale vacua and preventing the consistent realisation of the MPP in the 2HDM. The running of gauge, Yukawa and Higgs couplings in the MPP inspired 2HDM is described by a system of RG equations, which is basically the same as in the 2HDM of type II but with $\lambda_5 = 0$. The set of one-loop RG equations for the two Higgs doublet model with exact and softly broken Z_2 symmetry can be found in [2], [13]–[14].

For the purposes of our RG studies it is convenient to define

$$\rho_i(\mu) = \frac{\lambda_i(\mu)}{g_3^2(\mu)}, \quad \rho_t(\mu) = \frac{h_t^2(\mu)}{g_3^2(\mu)}, \quad R_i(\mu) = \frac{\rho_i(\mu)}{\rho_t(\mu)} = \frac{\lambda_i(\mu)}{h_t^2(\mu)}. \quad (9)$$

The vacuum stability constraints (8) and the MPP conditions (6)–(7) confine the allowed range of $R_i(\Lambda)$ in the vicinity of

$$R_1 = \frac{3}{4}, \quad R_2 = \frac{\sqrt{65} - 1}{8} \simeq 0.883, \quad R_3 = R_4 = 0, \quad (10)$$

which is a stable fixed point of the RG equations in the gaugeless limit ($g_i = 0$). Our numerical studies show that for $\Lambda = M_{Pl}$ and $R_1(M_{Pl}) = R_2(M_{Pl}) = R_0$ the value of R_0 can vary only within a very narrow interval from 0.79 to 0.87 if $h_t(\Lambda) \gtrsim 1.5$. Moreover the allowed range of R_0 shrinks significantly when $h_t(\Lambda)$ increases. For $h_t(\Lambda) \gtrsim 2.5$ the value of R_0 can only vary between 0.83 and 0.87. When the MPP scale decreases the allowed range of $\lambda_1(\Lambda)$ and $\lambda_2(\Lambda)$ enlarges.

Because in the MPP inspired 2HDM the $R_i(\Lambda)$ are confined near the fixed point (10), the corresponding solutions of the RG equations are attracted towards the invariant line that joins the stable fixed point in the gaugeless limit to the infrared stable fixed point

$$\rho_t = \frac{2}{9}, \quad \rho_1 = 0, \quad \rho_2 = \frac{\sqrt{689} - 25}{36} \simeq 0.0347, \quad \rho_3 = \rho_4 = 0, \quad (11)$$

where all the solutions of the RG equations are concentrated when the strong gauge coupling $g_3(\mu)$ approaches the Landau pole. As a result at the electroweak scale the solutions of the RG equations for the Higgs self-couplings are gathered in the vicinity of the quasi-fixed point, which is an intersection point of the invariant line and the Hill type effective surface [15]. Infrared fixed lines and surfaces as well as their properties were studied in detail in [16].

In Fig.2 we examine the RG running of the $\lambda_i(\mu)$. We set Λ equal to the Planck scale. Different curves in Fig.2 represent different solutions of the RG equations with boundary conditions satisfying Eqs. (6)–(7) where we keep $\lambda_1(\Lambda) = \lambda_2(\Lambda) = \lambda_0$. Because there is a stringent correlation between λ_0 and $h_t(\Lambda)$ we vary these couplings simultaneously, i.e. each curve below the quasi-fixed point solution corresponds to a particular set of λ_0 and $h_t(\Lambda)$ values. From Fig.2 one can see that at low energies the solutions of the RG equations for $\lambda_1(\mu)$, $\lambda_2(\mu)$ and $\lambda_3(\mu)$ are focused in a narrow interval near their quasi-fixed points. At the same time the solutions of the RG equations for $\lambda_4(\mu)$ are attracted to the corresponding quasi-fixed point rather weakly.

In Table 1 we specify the values of $\hat{\lambda}_i(M_t)$ to which the solutions of the RG equations converge at large $h_t(\Lambda)$. The set of $\hat{\lambda}_i(M_t)$ presented in Table 1 is obtained for $h_t^2(\Lambda) = 10$, $R_1(\Lambda) = 0.75$ and $R_2(\Lambda) \simeq 0.883$. The other Higgs self-couplings $\lambda_3(\Lambda)$ and $\lambda_4(\Lambda)$ are

determined from the MPP conditions (6)–(7). In Table 1 we present a few different sets of the Higgs self-couplings at the electroweak scale that correspond to different choices of the scale Λ between M_{Pl} and 10 TeV. The results given in Table 1 demonstrate that the absolute values of $\hat{\lambda}_i(M_t)$ increase as Λ approaches the electroweak scale. However the convergence of the Higgs self-couplings to $\hat{\lambda}_i(M_t)$ becomes weaker as the interval of evolution $t_0 = \ln(\Lambda^2/M_t^2)$ shrinks. In general the solutions of the RG equations for $\lambda_1(\mu)$ and $\lambda_2(\mu)$ are attracted to their quasi-fixed points much stronger than $\lambda_3(\mu)$ and $\lambda_4(\mu)$.

3. Higgs masses and couplings

Relying on the results of the analysis of the RG flow for the top quark Yukawa and Higgs couplings one can explore the Higgs spectrum in the MPP inspired 2HDM. The constraints on the Higgs masses in the 2HDM with unbroken Z_2 symmetry have been examined in a number of publications [14], [17]. The theoretical restrictions on the mass of the SM-like Higgs boson within the 2HDM with softly broken Z_2 symmetry were studied in [18]. The Higgs spectrum of the two Higgs doublet extension of the SM contains two charged and three neutral scalar states. Because in the MPP inspired 2HDM CP-invariance is preserved one of the neutral Higgs bosons is always CP-odd while two others are CP-even. The charged and pseudoscalar Higgs states gain masses

$$m_{\chi^\pm}^2 = m_A^2 - \frac{\lambda_4}{2}v^2, \quad m_A^2 = \frac{2m_3^2}{\sin 2\beta}. \quad (12)$$

The direct searches for the rare B-meson decays ($B \rightarrow X_s \gamma$) place a lower limit on the charged Higgs scalar mass in the 2HDM of type II [19]:

$$m_{\chi^\pm} > 350 \text{ GeV}, \quad (13)$$

which is also valid in our case.

The CP-even states are mixed and form a 2×2 mass matrix. The diagonalisation of this matrix gives

$$m_{h_1, h_2}^2 = \frac{1}{2} \left(M_{11}^2 + M_{22}^2 \mp \sqrt{(M_{22}^2 - M_{11}^2)^2 + 4M_{12}^4} \right). \quad (14)$$

$$M_{11}^2 = \left(\lambda_1 \cos^4 \beta + \lambda_2 \sin^4 \beta + \frac{\lambda}{2} \sin^2 2\beta \right) v^2,$$

$$M_{12}^2 = M_{21}^2 = \frac{v^2}{2} \left(-\lambda_1 \cos^2 \beta + \lambda_2 \sin^2 \beta + \lambda \cos 2\beta \right) \sin 2\beta,$$

$$M_{22}^2 = m_A^2 + \frac{v^2}{4} \left(\lambda_1 + \lambda_2 - 2\lambda \right) \sin^2 2\beta,$$

where $\lambda = \lambda_3 + \lambda_4$. The qualitative pattern of the Higgs spectrum depends very strongly on the mass of the pseudoscalar Higgs boson m_A . With increasing m_A the masses of all

the Higgs particles grow. At very large values of m_A ($m_A^2 \gg v^2$) the lightest Higgs boson mass m_{h_1} approaches its theoretical upper limit $\sqrt{M_{11}^2}$.

The upper bound on the mass of the lightest CP-even Higgs boson only depends on the Higgs self-couplings and $\tan \beta$. Therefore, using the results of our numerical studies of the RG flow presented in Table 1, one can calculate the theoretical restriction on m_{h_1} near the quasi-fixed point for each value of the MPP scale. The direct computations demonstrate that the allowed interval of variation of the lightest Higgs boson mass enlarges when Λ approaches the electroweak scale. The increase in the upper bound on m_{h_1} is caused by the growth of $\lambda_i(M_t)$ in the vicinity of the quasi-fixed point. In Fig. 3a we plot the theoretical restriction on the lightest Higgs boson mass m_{h_1} in the MPP inspired 2HDM as a function of scale Λ for $h_t^2(\Lambda) = 10$ and $h_t^2(\Lambda) = 2.25$. Fig. 3a illustrates that at high scale Λ the upper bound on m_{h_1} grows slightly with decreasing $h_t(\Lambda)$. When $\Lambda \simeq M_{Pl}$ the variation of $h_t^2(\Lambda)$ from 10 to 2.25 raises the theoretical limit on the mass of the SM-like Higgs boson from 110 GeV to 120 GeV. This indicates that in the MPP inspired 2HDM the scenarios with high scales Λ and large values of $h_t^2(\Lambda)$, $\lambda_1(\Lambda)$ and $\lambda_2(\Lambda)$ have not been entirely ruled out by unsuccessful Higgs searches at LEP. If $\Lambda \gtrsim 10^{10}$ GeV the lightest CP-even Higgs boson is lighter than 125 GeV. The upper bound on m_{h_1} grows from 125 GeV to 140 GeV on lowering the MPP scale from 10^{10} GeV to 10^7 GeV (see Fig. 3a and Table 1).

Stringent constraints coming from the direct Higgs searches at LEP suggest that the spectrum of Higgs bosons should be analysed together with the Higgs couplings to the gauge bosons and quarks. Such an analysis is especially important in the LHC era, because the same couplings determine the production cross sections and branching ratios of the Higgs particles at the LHC. Following the traditional notations we define normalised R -couplings of the neutral Higgs states to vector bosons as follows: $g_{VVh_i} = R_{VVh_i} \times \text{SM coupling}$ (i.e. $\frac{\bar{g}}{2} M_V$); $g_{ZAh_i} = \frac{\bar{g}}{2} R_{ZAh_i}$, where V is a W^\pm or a Z boson. The relative couplings R_{ZZh_i} and R_{ZAh_i} are given in terms of the angles α and β [21]:

$$\begin{aligned} R_{ZZh_1} &= R_{WWh_1} = -R_{ZAh_2} = \sin(\beta - \alpha), \\ R_{ZZh_2} &= R_{WWh_2} = R_{ZAh_1} = \cos(\beta - \alpha), \end{aligned} \quad (15)$$

where the angle α is defined as follows:

$$\begin{aligned} h_1 &= -(H_1^0 - v_1) \sin \alpha + (H_2^0 - v_2) \cos \alpha, \\ h_2 &= (H_1^0 - v_1) \cos \alpha + (H_2^0 - v_2) \sin \alpha, \\ \tan \alpha &= \frac{(\lambda v^2 - m_A^2) \sin \beta \cos \beta}{m_A^2 \sin^2 \beta + \lambda_1 v^2 \cos^2 \beta - m_{h_1}^2}. \end{aligned} \quad (16)$$

The absolute values of the R -couplings R_{VVh_i} and R_{ZAh_i} vary from zero to unity.

The couplings of the Higgs eigenstates to the top quark $g_{t\bar{t}h_i}$ can also be presented as a product of the corresponding SM coupling and the R -coupling $R_{t\bar{t}h_i}$:

$$R_{t\bar{t}h_1} = \frac{\cos \alpha}{\sin \beta}, \quad R_{t\bar{t}h_2} = \frac{\sin \alpha}{\sin \beta}. \quad (17)$$

Since the $R_{t\bar{t}h_i}$ are inversely proportional to $\sin \beta$ and near the quasi-fixed point $\tan \beta \lesssim 1$ (see Table 1), the values of $R_{t\bar{t}h_i}$ can be substantially larger than unity.

As follows from Eqs. (12)–(17), the spectrum and couplings of the Higgs bosons in the MPP inspired 2HDM are parametrized in terms of m_A , $\tan \beta$ and four Higgs self-couplings $\lambda_1(M_t)$, $\lambda_2(M_t)$, $\lambda_3(M_t)$ and $\lambda_4(M_t)$. Near the quasi-fixed points the Higgs self-couplings, the top quark Yukawa coupling and $\tan \beta$ have already been calculated (see Table 1). The numerical values of these couplings depend on the MPP scale. Therefore in the quasi-fixed point scenario all the Higgs masses and couplings can be considered as functions of the scale Λ and pseudoscalar mass m_A only.

In Fig. 3b–3d we examine the dependence of the Higgs masses and couplings on m_A for the MPP scale $\Lambda = 10$ TeV. From Fig. 3b it becomes clear that the masses of the heaviest CP-even and charged Higgs states rise with increasing pseudoscalar mass. At large values of m_A the corresponding Higgs states are almost degenerate around m_A . The lightest Higgs scalar h_1 is predominantly a SM-like Higgs boson, because its relative coupling to a Z pair is always close to unity (see Fig. 3c). As a result the non-observation of the SM-like Higgs particle at LEP rules out most of the parameter space near the quasi-fixed point if the scale Λ is relatively high, i.e. $\Lambda \gtrsim 10^{10}$ GeV. When the pseudoscalar mass is large ($m_A \gg M_t$) the interaction of the lightest CP-even Higgs state with the Higgs pseudoscalar and Z is suppressed.

The relative couplings of the CP-even Higgs bosons to the top quark change considerably when Λ varies. When Λ is near the Planck scale the lightest CP-even Higgs eigenstate is predominantly composed of H_1^0 . Therefore its coupling to the top quark is typically smaller than the coupling of the heaviest one. However at low values of the MPP scale, $\Lambda < 10^6$ GeV, the lightest CP-even Higgs state is dominated by H_2^0 . As follows from Fig. 3d this leads to a substantial increase of the coupling of the lightest Higgs scalar to the top quark. Our numerical studies demonstrate that, due to the significant growth of $R_{t\bar{t}h_1}$, the production cross section of the SM-like Higgs in the 2HDM can be 1.5 – 2 times larger than in the SM. With increasing m_A the heaviest CP-even, CP-odd and charged Higgs states decouple and the coupling of the lightest Higgs scalar to the top quark approaches the SM one. Nevertheless the enhanced production of the SM-like Higgs boson allows us to distinguish the quasi-fixed point scenario in the MPP inspired 2HDM with low MPP scale from the SM and its supersymmetric extensions, even if extra Higgs states are relatively heavy ($m_A \gtrsim 500 - 700$ GeV).

4. Conclusions

We have studied the RG flow of $h_t(\mu)$ and $\lambda_i(\mu)$, as well as the Higgs spectrum and couplings, within the simplest two Higgs doublet extension of the SM — the MPP inspired 2HDM. When $h_t(\Lambda) \gtrsim 1$ the solutions of the RG equations for the top quark Yukawa coupling are concentrated in the vicinity of the quasi-fixed point at the electroweak scale. Then the value of $\tan\beta$ can be chosen so that the correct value of the running top quark mass is reproduced. In the MPP inspired 2HDM the values of $h_t(M_t)$ and $\tan\beta$ corresponding to the quasi-fixed point depend mainly on the MPP scale Λ . We have argued that, at large values of $h_t(\Lambda)$, the MPP and vacuum stability conditions constrain the Higgs self-couplings at the MPP scale very strongly. When the scale Λ is high enough the $\lambda_i(\Lambda)$ are confined in a narrow region near a point corresponding to a fixed point of the RG equations in the gaugeless limit ($g_i = 0$). This ensures the convergence of the solutions for $\lambda_1(\mu)$ and $\lambda_2(\mu)$ to the quasi-fixed points. Two other non-zero Higgs self-couplings $\lambda_3(\mu)$ and $\lambda_4(\mu)$ are attracted considerably weaker to the quasi-fixed points.

The qualitative pattern of the Higgs spectrum in the MPP inspired 2HDM is determined by the mass of the pseudoscalar Higgs boson m_A . When $m_A \gg M_t$ the masses of the charged, CP-odd and heaviest CP-even Higgs bosons are almost degenerate around m_A . In the considered limit the lightest CP-even Higgs boson mass m_{h_1} attains its maximal value. Using the results of our analysis of the RG flow of the Higgs and Yukawa couplings, we have examined the dependence of the upper bound on m_{h_1} near the quasi-fixed point on the scale Λ . If $\Lambda \gtrsim 10^{10}$ GeV the mass of the lightest Higgs particle does not exceed 125 GeV. However at low MPP scale $\Lambda \simeq 10 - 100$ TeV the upper bound on m_{h_1} reaches 200 – 220 GeV. The lightest Higgs scalar in the considered case is predominantly a SM-like Higgs boson, since its relative coupling to a Z pair is rather close to unity. Nevertheless at low MPP scales the quasi-fixed point scenario leads to large values of the relative coupling of the lightest Higgs scalar to the top quark, resulting in the enhanced production of this particle at the LHC. Thus the analysis of production and decay rates of the SM-like Higgs boson at the LHC should make possible the distinction between the quasi-fixed point scenario in the MPP inspired 2HDM with low scale Λ , the SM and the MSSM even if extra Higgs states are relatively heavy, i.e. $m_A \simeq 500 - 700$ GeV.

Acknowledgements

The authors are grateful to L. V. Laperashvili and M. Sher for valuable comments and remarks. RN would also like to thank A. Djouadi, J. F. Gunion, D. J. Miller, J. Kalinowski, D. I. Kazakov, S. F. King, M. Shifman and P. M. Zerwas for fruitful discussions. The authors acknowledge support from the SHEFC grant HR03020 SUPA 36878.

References

- [1] C. T. Hill, Phys. Rev. D **24** (1981) 691.
- [2] C. T. Hill, C. N. Leung and S. Rao, Nucl. Phys. B **262** (1985) 517;
- [3] M. Sher, Phys. Rep. **179** (1989) 273; J. F. Gunion, H. E. Haber, G. Kane, S. Dawson, *The Higgs Hunter's Guide*, (Addison–Wesley, Redwood City, CA, 1990).
- [4] E. Brubaker *et al.* [Tevatron Electroweak Working Group], hep-ex/0608032.
- [5] B. Brahmachari, Mod. Phys. Lett. A **12** (1997) 1969; J. A. Casas, J. R. Espinosa and H. E. Haber, Nucl. Phys. B **526** (1998) 3.
- [6] G. K. Yeghiyan, M. Jurčišin and D. I. Kazakov, Mod. Phys. Lett. A **14** (1999) 601; S. Codoban, M. Jurcisin and D. Kazakov, Phys. Lett. B **477** (2000) 223.
- [7] C. D. Froggatt, I. G. Knowles and R. G. Moorhouse, Phys. Lett. B **298** (1993) 356; V. Barger, M. S. Berger, P. Ohmann and J. N. Phillips, Phys. Lett. B **314** (1993) 351; M. Carena, M. Olechowski, S. Pokorski, and C. E. M. Wagner, Nucl. Phys. B **419** (1994) 213; V. Barger, M. S. Berger and P. Ohmann, Phys. Rev. D **49**, 4908 (1994); W. A. Bardeen, M. Carena, S. Pokorski, and C. E. M. Wagner, Phys. Lett. B **320** (1994) 110; M. Carena, M. Olechowski, S. Pokorski and C. E. M. Wagner, Nucl. Phys. B **426** (1994) 269; M. Carena and C. E. M. Wagner, Nucl. Phys. B **452** (1995) 45; S. A. Abel and B. C. Allanach, Phys. Lett. B **415** (1997) 71; S. A. Abel and B. C. Allanach, Phys. Lett. B **431** (1998) 339; M. Jurčišin and D. I. Kazakov, Mod. Phys. Lett. A **14** (1999) 671.
- [8] J. Bagger, S. Dimopoulos and E. Masso, Phys. Lett. B **156** (1985) 357; C. D. Froggatt, I. G. Knowles and R. G. Moorhouse, Phys. Lett. B **249** (1990) 273; C. D. Froggatt, I. G. Knowles and R. G. Moorhouse, Nucl. Phys. B **386** (1992) 63.
- [9] D. L. Bennett, H. B. Nielsen and I. Picek, Phys. Lett. B **208** (1988) 275; D. L. Bennett, H. B. Nielsen, Int. J. Mod. Phys. A **9** (1994) 5155; *ibid* **14**, 3313 (1999); D. L. Bennett, C. D. Froggatt, H. B. Nielsen, in *Proceedings of the 27th International Conference on High Energy Physics, Glasgow, Scotland, 1994*, p.557; D. L. Bennett and H. B. Nielsen, in *Proceedings of the 28th International Conference on High-energy Physics, Warsaw, Poland, 1996*, p.1646; D. L. Bennett, hep-ph/9607341;
- [10] C. D. Froggatt, L. V. Laperashvili, R. B. Nevzorov, H. B. Nielsen and M. Sher, hep-ph/0412333; C. D. Froggatt, L. Laperashvili, R. Nevzorov, H. B. Nielsen and M. Sher, Phys. Rev. D **73** (2006) 095005.

- [11] C. D. Froggatt, R. Nevzorov, H. B. Nielsen and D. Thompson, arXiv:0806.3190 [hep-ph].
- [12] R. Tarrach, Nucl. Phys. B **183** (1981) 384; N. Gray, D. J. Broadhurst, W. Grafe and K. Schilcher, Z. Phys. C **48** (1990) 673; D. J. Broadhurst, N. Gray and K. Schilcher, Z. Phys. C **52** (1991) 111; K. G. Chetyrkin and M. Steinhauser, Phys. Rev. Lett. **83** (1999) 4001; K. G. Chetyrkin and M. Steinhauser, Nucl. Phys. B **573** (2000) 617.
- [13] K. Inoue, A. Kakuto, Y. Nakano, Prog. Theor. Phys. **63** (1980) 234; H. E. Haber, R. Hempfling, Phys. Rev. D **48** (1993) 4280.
- [14] H. Komatsu, Prog. Theor. Phys. **67** (1982) 1177; D. Kominis, R. S. Chivukula, Phys. Lett. B **304** (1993) 152.
- [15] R. B. Nevzorov and M. A. Trusov, Phys. Atom. Nucl. **64** (2001) 1299 [Yad. Fiz. **64** (2001) 1375]; R. B. Nevzorov and M. A. Trusov, Phys. Atom. Nucl. **65** (2002) 335 [Yad. Fiz. **65** (2002) 359]; R. B. Nevzorov, K. A. Ter-Martirosyan and M. A. Trusov, arXiv:hep-ph/0301068.
- [16] B. Schrempp and F. Schrempp, Phys. Lett. B **299** (1993) 321; B. Schrempp, Phys. Lett. B **344** (1995) 193; B. Schrempp and M. Wimmer, Prog. Part. Nucl. Phys. **37** (1996) 1.
- [17] R. Flores, M. Sher, Ann. Phys. **148** (1983) 295; A. Bovier, D. Wyler, Phys. Lett. B **154** (1985) 43; A. J. Davies, G. C. Joshi, Phys. Rev. Lett. **58** (1987) 1919; J. Maalampi, J. Sirkka, I. Vilja, Phys. Lett. B **265** (1991) 371; S. Kanemura, T. Kubota, E. Takasugi, Phys. Lett. B **313** (1993) 155; S. Nie and M. Sher, Phys. Lett. B **449** (1999) 89; A. G. Akeroyd, A. Arhrib, E. Naimi, Phys. Lett. B **490** (2000) 119.
- [18] S. Kanemura, T. Kasai and Y. Okada, Phys. Lett. B **471** (1999) 182.
- [19] M. Ciuchini, G. Degrossi, P. Gambino, G. F. Giudice, Nucl. Phys. B **527** (1998) 21; P. Gambino, M. Misiak, Nucl. Phys. B **611** (2001) 338.
- [20] P. A. Kovalenko, R. B. Nevzorov and K. A. Ter-Martirosian, Phys. Atom. Nucl. **61** (1998) 812 [Yad. Fiz. **61** (1998) 898]; R. B. Nevzorov and M. A. Trusov, J. Exp. Theor. Phys. **91** (2000) 1079 [Zh. Eksp. Teor. Fiz. **91** (2000) 1251]; R. B. Nevzorov, K. A. Ter-Martirosyan and M. A. Trusov, Phys. Atom. Nucl. **65** (2002) 285 [Yad. Fiz. **65** (2002) 311].
- [21] *For a recent review, see:* M. Carena and H. E. Haber, Prog. Part. Nucl. Phys. **50** (2003) 63.

Table 1. The top quark Yukawa and Higgs couplings, $\tan \beta$ and the upper bound on the lightest Higgs boson mass corresponding to the quasi-fixed point scenario in the MPP inspired 2HDM (all mass parameters are given in GeV).

Λ	$\hat{h}_t(M_t)$	$\tan \beta$	$\hat{\lambda}_1(M_t)$	$\hat{\lambda}_2(M_t)$	$\hat{\lambda}_3(M_t)$	$\hat{\lambda}_4(M_t)$	m_{h_1}
M_{Pl}	1.26	1.08	0.41	0.94	0.037	-0.33	114
10^{16}	1.30	1.02	0.48	1.02	0.038	-0.36	115
10^{13}	1.36	0.94	0.57	1.15	0.035	-0.40	118
10^{10}	1.45	0.84	0.73	1.36	0.019	-0.49	124
10^7	1.61	0.71	1.05	1.78	-0.057	-0.67	143
10^4	2.05	0.51	2.09	3.09	-0.65	-1.21	226

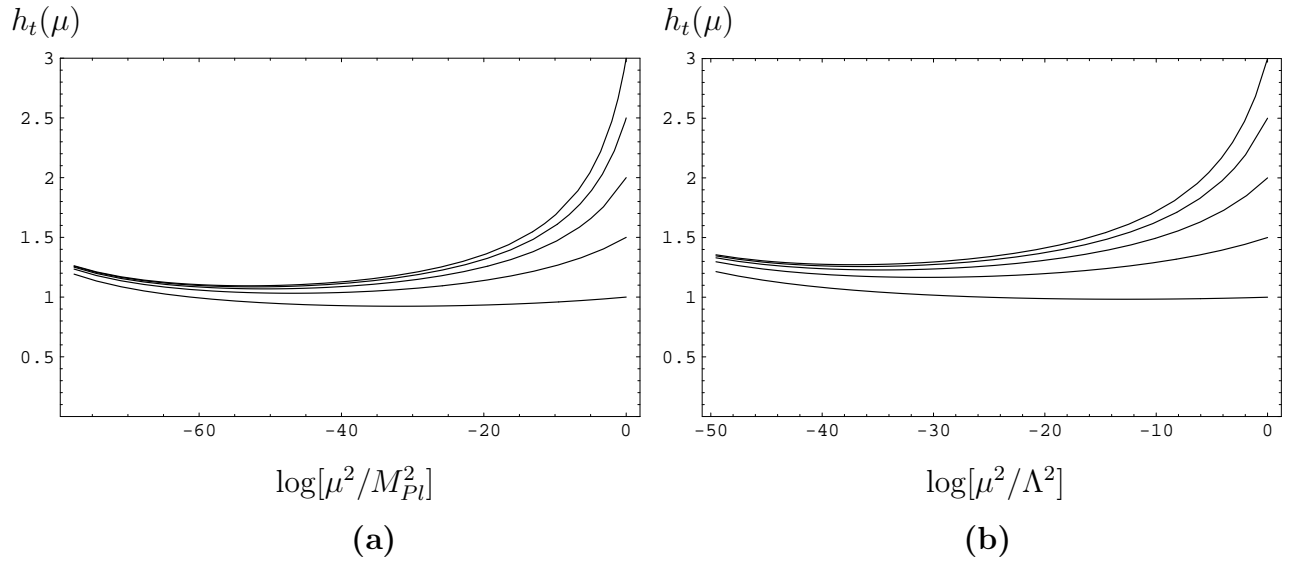


Figure 1: The RG flow of the top quark Yukawa coupling for (a) $\Lambda = M_{Pl}$ and (b) $\Lambda = 10^{13}$ GeV. The value of $\alpha_3(M_Z)$ is set equal to 0.117.

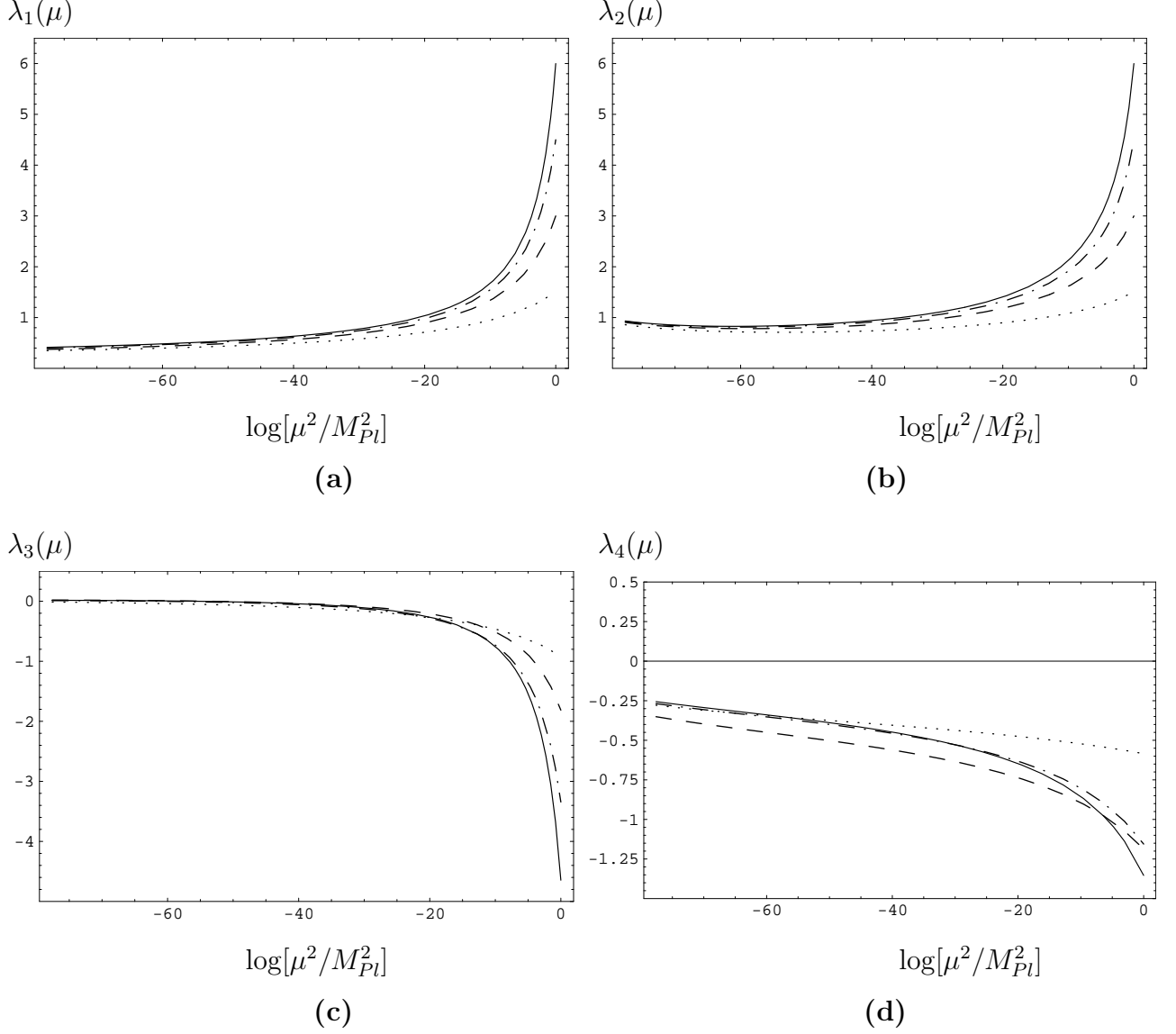


Figure 2: The RG flow of the Higgs self-couplings within the MPP inspired 2HDM: (a) $\lambda_1(\mu)$; (b) $\lambda_2(\mu)$; (c) $\lambda_3(\mu)$; (d) $\lambda_4(\mu)$. The solid, dash-dotted, dashed and dotted lines correspond to different sets of $(h_t(\Lambda), \lambda_1(\Lambda) = \lambda_2(\Lambda) = \lambda_0)$, i.e. $(2.65, 6)$, $(2.3, 4.5)$, $(1.9, 3)$ and $(1.35, 1.5)$ respectively, while $\lambda_3(\Lambda)$ and $\lambda_4(\Lambda)$ are chosen so that the MPP conditions are fulfilled.

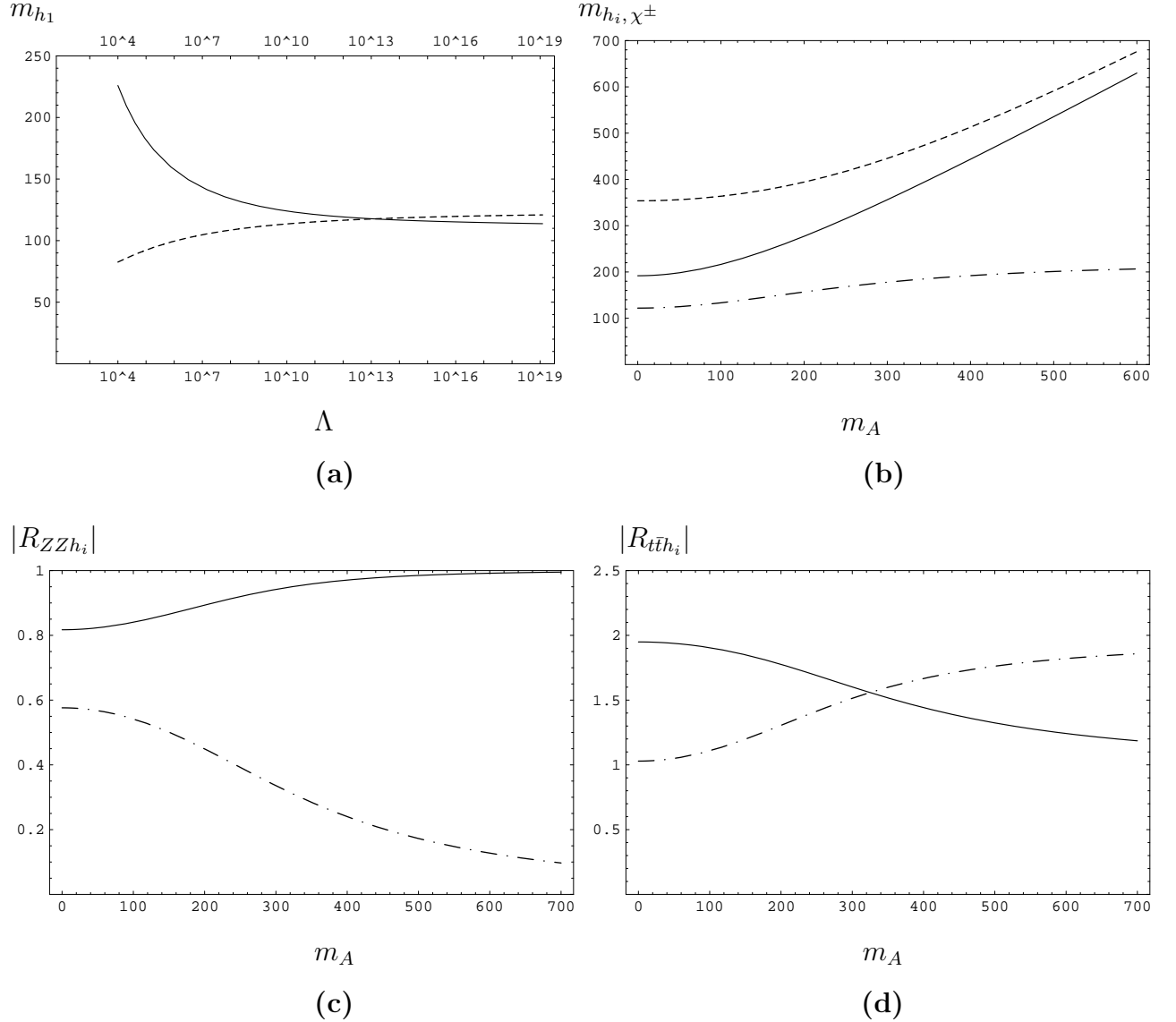


Figure 3: Higgs masses and couplings near the quasi-fixed point in the MPP inspired 2HDM. (a) Upper bound on the mass of the SM-like Higgs boson versus MPP scale Λ in the quasi-fixed point scenario. The solid and dashed curves correspond to $h_t^2(\Lambda) = 10$ and $h_t^2(\Lambda) = 2.25$. (b) Spectrum of Higgs bosons versus m_A for $\Lambda = 10$ TeV and $h_t^2(\Lambda) = 10$. The dash-dotted and dashed lines correspond to the CP-even Higgs boson masses, while the solid line represents the mass of the charged Higgs states. (c) Absolute values of the relative couplings R_{ZZi} of the Higgs scalars to a Z pair. Solid and dashed-dotted curves represent the dependence of the couplings of the lightest and heaviest CP-even Higgs states to a Z pair on m_A . The parameters are the same as in (b). (d) Absolute values of the relative couplings $R_{t\bar{t}i}$ of the lightest (solid curve) and heaviest (dashed-dotted curve) CP-even Higgs bosons to the top quark as a function of m_A . The parameters are the same as in (b)–(c). All mass parameters are given in GeV.